

Published in final edited form as:

*Nat Cell Biol.* 2007 April ; 9(4): 445–452. doi:10.1038/ncb1556.

## Uncoupling proteins 2 and 3 are fundamental for mitochondrial $\text{Ca}^{2+}$ uniport

Michael Trenker<sup>#1</sup>, Roland Malli<sup>#1</sup>, Ismene Fertschai<sup>1</sup>, Sanja Levak-Frank<sup>1</sup>, and Wolfgang F. Graier<sup>#1,3</sup>

<sup>1</sup>Institute of Molecular Biology and Biochemistry, Centre of Molecular Medicine, Medical University of Graz, Harrachgasse 21/III, 8010 Graz, Austria

# These authors contributed equally to this work.

### Abstract

Mitochondrial  $\text{Ca}^{2+}$  uptake is crucial for the regulation of the rate of oxidative phosphorylation<sup>1</sup>, the modulation of spatiotemporal cytosolic  $\text{Ca}^{2+}$  signals<sup>2,3,4</sup> and apoptosis<sup>5</sup>. Although the phenomenon of mitochondrial  $\text{Ca}^{2+}$  sequestration, its characteristics and physiological consequences have been convincingly reported<sup>6,7</sup>, the actual protein(s) involved in this process are unknown. Here, we show that the uncoupling proteins 2 and 3 (UCP2 and UCP3) are essential for mitochondrial  $\text{Ca}^{2+}$  uptake. Using overexpression, knockdown (small interfering RNA) and mutagenesis experiments, we demonstrate that UCP2 and UCP3 are elementary for mitochondrial  $\text{Ca}^{2+}$  sequestration in response to cell stimulation under physiological conditions — observations supported by isolated liver mitochondria of *Ucp2*<sup>-/-</sup> mice lacking ruthenium red-sensitive  $\text{Ca}^{2+}$  uptake. Our results reveal a novel molecular function for UCP2 and UCP3, and may provide the molecular mechanism for their reported effects<sup>8-10</sup>. Moreover, the identification of proteins fundamental for mitochondrial  $\text{Ca}^{2+}$  uptake expands our knowledge of the physiological role for mitochondrial  $\text{Ca}^{2+}$  sequestration.

---

Uncoupling proteins (UCPs) are embedded in the inner mitochondrial membrane and belong to the superfamily of mitochondrial ion transporters<sup>11</sup>. UCP1, which is preferentially expressed in brown adipose tissue, accounts for heat production by inducing a  $\text{H}^+$  leak that uncouples oxidative phosphorylation. In contrast, the physiological function of the family members UCP2 and UCP3, which have been identified in many tissues<sup>11</sup>, is still a matter of debate. Despite the fact that both proteins promote  $\text{H}^+$  influx in isolated mitochondria under specific conditions, their involvement in heat production has not been confirmed to date (for review see ref. 10). UCP2- and UCP3-related proteins also exist in ectothermic fish and plants, which do not require thermogenesis, emphasizing that additional functions of these UCPs may exist. Consistently, evidence has accumulated that points to their contribution in

---

© 2007 Nature Publishing Group

<sup>3</sup>Correspondence should be addressed to W.F.G. (wolfgang.graier@meduni-graz.at).

**AUTHOR CONTRIBUTIONS:** All authors designed this work. M.T. cloned all constructs, designed siRNAs and performed western blots, tissue isolation and  $\text{Ca}^{2+}$  measurements. I.F. isolated single mitochondria. S.L.-F. was responsible for breeding the knockout mice. R.M. performed the image analyses and ATP measurements and, together with W.F.G., who wrote the paper, initiated and guided this study. All authors discussed the results and commented on the manuscript.

**COMPETING FINANCIAL INTERESTS@** The authors declare that they have no competing financial interests.

many cellular processes, such as mitochondrial free-radical production<sup>12</sup>, apoptosis<sup>13</sup>, the regulation of hormone secretion (UCP2)<sup>14</sup>, and glucose and fatty acid metabolism (UCP3)<sup>15</sup>. However, the reported smooth uncoupling by UCP2 and UCP3 (ref. 12) seems unlikely to account exclusively for such variety of functions. As, in contrast with H<sup>+</sup>, Ca<sup>2+</sup> is known to control a large amount of biological processes, we assessed the involvement of UCP2 and UCP3 in mitochondrial Ca<sup>2+</sup> homeostasis.

Initially, expression of UCPs was evaluated in endothelial cells. Using RT-PCR (Fig. 1A) and western blot analyses (Fig. 2a), the expression of UCP2 and/or UCP3, but not UCP1, could be verified in the human umbilical vein-derived cell line EA.hy926 (ref. 16; Fig. 1A), as well as in various human cell lines and short-term cultured human umbilical vein endothelial cells (see Supplementary Information, Fig S1a). After cloning and sequence verification, respective fluorescent fusion proteins of UCP2 (gi13259540) and UCP3 (gi13259544) were constructed and expressed in endothelial cells, where they revealed exclusive mitochondrial targeting (Fig. 1B). Subsequently, the consequences of overexpression of UCP2 or UCP3 on mitochondrial Ca<sup>2+</sup> signalling were assessed in single cells expressing the mitochondrial-targeted Ca<sup>2+</sup> sensor ratiometric pericam<sup>17</sup>, which exhibited identical dynamics (that is, maximum, minimum; see Supplementary Information, Fig. S1c) regardless of the protein levels of the UCPs. Overexpression of the proteins alone did not affect basic parameters that may influence the ability of the mitochondria to sequester Ca<sup>2+</sup> — such as the architectural organization of the mitochondria (Fig. 1B and see Supplementary Information, Fig. S1b, e), their motility (see Supplementary Information, Movie 1), matrix pH (see Supplementary Information, Fig. S1c) and membrane potential (see Supplementary Information, Fig. S1d), basal ATP production (see Supplementary Information, Fig. S1e) or focal contacts with the endoplasmic reticulum (see Supplementary Information, Fig. S1b, f). In line with these findings, basal Ca<sup>2+</sup> concentration in the mitochondria ([Ca<sup>2+</sup>]<sub>mito</sub>; see Supplementary Information, Table S1) and the endoplasmic reticulum, and histamine-induced endoplasmic reticulum Ca<sup>2+</sup> release (see Supplementary Information, Fig. S1g) were not affected by overexpression of UCP2 or UCP3. Remarkably, despite identical cytoplasmic Ca<sup>2+</sup> elevation in response to histamine in cells transiently over-expressing UCP2 or UCP3 (see Supplementary Information, Fig. S1h), mitochondrial Ca<sup>2+</sup> sequestration was enhanced by 33 and 76%, respectively (Fig. 1C). In contrast, overexpression of UCP2 or UCP3 did not affect changes in the primarily pH-sensitive pericam fluorescence at 485 nm (Fig. 1D). Notably, the kinetics of mitochondrial Ca<sup>2+</sup> removal after agonist washout was slightly faster in UCP-overexpressing cells (control,  $-0.073 \pm 0.030$ ,  $n = 32$ ; UCP2,  $-0.085 \pm 0.020$ ,  $n = 23$ , not significant (n.s.) versus control; UCP3,  $-0.108 \pm 0.026$  [ $1-(F_{433}/F_0)/\text{min}$ ],  $n = 19$ ,  $P < 0.05$  versus control), thus, indicating that the enhanced mitochondrial Ca<sup>2+</sup> accumulation during cell stimulation is most likely due to increased mitochondrial Ca<sup>2+</sup> uptake, but not to a decreased mitochondrial Ca<sup>2+</sup> extrusion. In line with these findings, overexpression of UCP2 and UCP3 strongly increased mitochondrial Ca<sup>2+</sup> sequestration on Ca<sup>2+</sup> entry (see Supplementary Information, Fig. S1i).

Identical findings were obtained in HeLa and CHO-K1 cells that were stimulated with 100  $\mu\text{M}$  histamine or 10  $\mu\text{M}$  ATP, respectively (see Supplementary Information, Fig. S1j), suggesting that the reported feature of UCP2 and UCP3 represents a ubiquitous

phenomenon. These findings are consistent with earlier reports that UCP3 overexpression increased mitochondrial susceptibility to  $\text{Ca}^{2+}$ -dependent opening of the permeability transition pore in permeabilized HEK293 cells<sup>13</sup>. However, in intact cells, overexpression of UCP2 or UCP3 did not initiate opening of a cyclosporin A-sensitive transition pore on cell stimulation (data not shown), possibly due to the intact mitochondrial environment, which limits excessive mitochondrial  $\text{Ca}^{2+}$  overload.

Remarkably, expression of UCP1 in endothelial cells that do not constitutively express this protein had no effect on basal mitochondrial  $\text{Ca}^{2+}$  content, and did not alter mitochondrial  $\text{Ca}^{2+}$  sequestration on cell stimulation (see Supplementary Information, Fig. S1k). These data further confirm the concept that UCP2 and UCP3 exhibit different physiological functions than UCP1, and indicate that strong expression of an inner mitochondrial protein does not mimic the effect of UCP2 and UCP3 on mitochondrial  $\text{Ca}^{2+}$  permeability.

To explore the contribution of UCP2 and UCP3 to mitochondrial  $\text{Ca}^{2+}$  sequestration, the impact of UCP overexpression on the sensitivity and capacity of the mitochondrial  $\text{Ca}^{2+}$  uptake machinery was assessed by measuring the concentration-response relationship to histamine. These experiments revealed that overexpression of UCP2 and UCP3 increased the capacity of mitochondrial  $\text{Ca}^{2+}$  uptake (Fig. 1E), whereas the affinity to histamine-induced cytosolic  $\text{Ca}^{2+}$  elevations, which were not altered by the UCP overexpression (see Supplementary Information, Fig. S1l), remained unaffected ( $\text{EC}_{50}$ -histamine: control, 7.73 (4.96–11.74)  $\mu\text{M}$ ; UCP2, 5.35 (3.26–8.77)  $\mu\text{M}$ ; UCP3, 4.40 (2.44–7.93)  $\mu\text{M}$ ; Fig. 1E).

Under physiological conditions, the extent of  $\text{Ca}^{2+}$  actually sequestered by the mitochondria strictly depends on the mitochondrial membrane potential<sup>5</sup>. Thus, it seemed possible that, on cell stimulation, UCP2 and UCP3 affect the bioenergetic status of the mitochondria, which results in an augmented capability of mitochondria to take up  $\text{Ca}^{2+}$ . To explore this possibility, mitochondria were completely de-energized and/or depolarized using 2  $\mu\text{M}$  carbonyl cyanide-4-trifluoromethoxyphenylhydrazone (FCCP; a concentration suitable for complete depolarization of the mitochondria; see Supplementary Information, Fig. S1m) and 2  $\mu\text{M}$  oligomycin, thus providing a condition in which the uptake of  $\text{Ca}^{2+}$  into the mitochondria is not energetic anymore and, therefore, exclusively follows the concentration gradient of this ion. Unsurprisingly, mitochondrial  $\text{Ca}^{2+}$  sequestration was largely reduced under these conditions and exhibited only approximately 20% of that obtained under control conditions (Fig. 1F). Nevertheless, overexpression of UCP2 or UCP3 strongly augmented mitochondrial  $\text{Ca}^{2+}$  uptake on maximal cell stimulation with 100  $\mu\text{M}$  histamine and 15  $\mu\text{M}$  2,5-di-*tert*-butylhydroquinone (BHQ), even under these depolarizing conditions (Fig. 1F). As these experiments were performed in the presence of 10  $\mu\text{M}$  CGP 37157, an inhibitor of mitochondrial  $\text{Na}^{+}$ - $\text{Ca}^{2+}$  exchanger ( $\text{NCX}_{\text{mito}}$ )<sup>2</sup>, the obtained amplification of mitochondrial  $\text{Ca}^{2+}$  uptake cannot be due to the reversed mode activity of  $\text{NCX}_{\text{mito}}$ , and supports the concept that UCP2 and UCP3 inherently accomplish mitochondrial  $\text{Ca}^{2+}$  uptake.

Notably, in contrast with the  $\text{H}^{+}$  conductance of UCP2 and UCP3 — which was found only on exposure to products of reactive oxygen species (ROS) metabolism, such as hydroxynonenal and, perhaps, fatty acids<sup>8</sup> — our data suggest that these UCP orthologues achieve  $\text{Ca}^{2+}$  sequestration into mitochondria without any additional pre-activation. Thus, a

fundamental role for UCP2 and UCP3 in the phenomenon of mitochondrial  $\text{Ca}^{2+}$  sequestration is emphasized.

To challenge this hypothesis, loss-of-function experiments were conducted using selective siRNA against *UCP2* and *UCP3* (see Supplementary Information, Fig. S2a). Compared with non-transfected controls and siRNA controls, siRNAs against *UCP2* and *UCP3* strongly reduced expression of the respective protein (Fig. 2a). Remarkably, in cells that were transfected with siRNA against either *UCP2* or *UCP3*, mitochondrial  $\text{Ca}^{2+}$  uptake in response to histamine was strongly reduced (Fig. 2b), whereas cytosolic  $\text{Ca}^{2+}$  elevation was not altered (see Supplementary Information, Fig. S2b). As the efficiency of siRNA knockdown of the respective proteins varies depending on multiple factors, the effect of siRNAs against *UCP2* and *UCP3* on mitochondrial  $\text{Ca}^{2+}$  sequestration was demonstrated by plotting the distribution of the effects achieved in the individual experiments (Fig. 2b). Consistent with our overexpression experiments (Fig. 1C), siRNA against *UCP3* diminished mitochondrial  $\text{Ca}^{2+}$  signalling to a greater extent than silencing of *UCP2*, suggesting that UCP3 more efficiently sequesters  $\text{Ca}^{2+}$  into the mitochondria than UCP2. Remarkably, double transfection of endothelial cells with the siRNAs against *UCP2* and *UCP3* yielded further reduction of mitochondrial  $\text{Ca}^{2+}$  elevation. Two-thirds of cells cotransfected with siRNAs against *UCP2* and *UCP3* exhibited a reduction in mitochondrial  $\text{Ca}^{2+}$  signalling greater than 80% of that achieved in control cells (Fig. 2b). In addition, similar experiments were performed in HeLa cells that express UCP3 but not UCP2 (see Supplementary Information, Fig. S1a): transfection with siRNA against *UCP2* had no effect on mitochondrial  $\text{Ca}^{2+}$  elevation in response to histamine, whereas in cells transfected with siRNA against *UCP3*, mitochondrial  $\text{Ca}^{2+}$  elevation was diminished, or even abolished, in comparison with the respective control (Fig. 2c). Moreover, mitochondrial  $\text{Ca}^{2+}$  uptake in intact (Fig. 2d) and permeabilized (Fig. 2e) HeLa cells that were transiently transfected with siRNA against *UCP3*, could be rescued by cotransfection with UCP2.

To further support our concept of an elementary contribution of these UCP isoforms to mitochondrial  $\text{Ca}^{2+}$  uniport,  $\text{Ca}^{2+}$  uptake experiments were performed in liver mitochondria (Fig. 3) isolated from *Ucp2*<sup>-/-</sup> mice<sup>18</sup> and their wild-type littermates. In liver, *Ucp2* was found to represent the only UCP isoform<sup>19</sup>, and thus mitochondria from this tissue are suitable to facilitate determination of the consequence of *Ucp2* knockout on the  $\text{Ca}^{2+}$  uptake of the organelle. In suspended mitochondria isolated from wild-type littermates, mitochondria exhibited a strong  $\text{Ca}^{2+}$  uptake from medium that was diminished by approximately 41% with 100 nM ruthenium red (Fig. 3a, c). In contrast, uptake of extra-mitochondrial  $\text{Ca}^{2+}$  by suspended mitochondria isolated from *Ucp2*<sup>-/-</sup> mice was reduced by approximately 53% compared with that observed in wild-type mitochondria, whereas 100 nM ruthenium red had no further effect (Fig. 3b, c). The remaining  $\text{Ca}^{2+}$  uptake in mitochondria isolated from *Ucp2*<sup>-/-</sup> mice, or in the presence of ruthenium red, may be due to alternative  $\text{Ca}^{2+}$  uptake pathway(s) under these conditions (for example,  $\text{Ca}^{2+}$ - $\text{H}^+$  or  $\text{Na}^+$ - $\text{Ca}^{2+}$  exchanger). Therefore, comparable data were obtained in single mitochondria isolated from wild-type and *Ucp2*<sup>-/-</sup> mice, and further confirmed the complete lack of ruthenium red-sensitive  $\text{Ca}^{2+}$  uptake in liver mitochondria from *Ucp2*<sup>-/-</sup> animals (Fig. 3d–g).

Expression of UCP2 and UCP3 in the yeast *Saccharomyces cerevisiae* did not affect mitochondrial membrane potential and  $\text{Ca}^{2+}$  sequestration, which was insensitive to ruthenium red (see Supplementary Information, Fig. S3). These data indicate that in freshly isolated single mitochondria of these yeast strains, no ruthenium red-sensitive  $\text{Ca}^{2+}$  uptake exists and that UCP2 or UCP3 alone are not suitable to establish this phenomenon in this heterologous environment.

Although UCP2 and UCP3, which are approximately 72% homologous, share approximately 58% protein homology with UCP1 (see Supplementary Information, Fig. S4a), there is a wide consensus that these orthologues do not exhibit a thermogenetic function like UCP1. Thus, it was expected that the domain that is crucial for the  $\text{Ca}^{2+}$  conductance of UCP2 and UCP3 would be localized in regions with high homology between UCP2 and UCP3, but not with UCP1. Using sequence-based annotation analysis, the protonated *A-R-E-E* domain of UCP2 and UCP3 in the second inter-membrane loop was identified as differing from the polar *A-T-T-E* sequence of UCP1 (Fig. 4a). It is predicted that this domain forms a helix that is localized at the matrix side of the inner mitochondrial membrane (Fig. 4b). Mutagenesis of this domain (Fig. 4a) slightly shortened the respective helix, but no other effect on the structure of the protein was predicted (Fig. 4b). The localization of UCP2 and UCP3 mutants did not differ from that of their non-mutant analogues (see Supplementary Information, Fig. S4b). In functional experiments, overexpression of the mutants of UCP2 or UCP3 in endothelial cells failed to result in increased mitochondrial  $\text{Ca}^{2+}$  sequestration, but counteracted the constitutive  $\text{Ca}^{2+}$  uptake and allowed only a reduced and transient  $\text{Ca}^{2+}$  elevation compared with control cells (Fig. 4c). In HeLa cells, which express UCP3 but not UCP2 (see Supplementary Information, Fig. S1a), the UCP2 mutant failed to rescue mitochondrial  $\text{Ca}^{2+}$  uptake if *UCP3* expression was knocked down with siRNA, and diminished the activity of constitutive UCP3 for  $\text{Ca}^{2+}$  sequestration (Fig. 4d). These data suggest that, despite their correct targeting, mutated UCP2 and UCP3 exhibit very little or no functional activity for mitochondrial  $\text{Ca}^{2+}$  uptake. In addition, as the mutated UCP2 interfered with constitutive (functional) UCP3 in HeLa cells, and given our findings that overexpression of UCP2 or UCP3 alone was suitable for elevating mitochondrial  $\text{Ca}^{2+}$  uptake, we speculate that these proteins form homo- and hetero-multimers to contribute to the mitochondrial  $\text{Ca}^{2+}$  uniporter, which becomes inactive if a mutated UCP2 or UCP3 is co-assembled.

As mitochondrial  $\text{Ca}^{2+}$  uptake has been shown to trigger agonist-induced ATP synthesis in mitochondria<sup>1</sup>, agonist-induced mitochondrial ATP production can be used as an indirect measure of mitochondrial  $\text{Ca}^{2+}$  sequestration. Therefore, to investigate the physiological consequences of UCP2 and UCP3 activity, mitochondrial ATP synthesis was measured in cells overexpressing either UCP2 or UCP3. Notably, if these UCP orthologues exhibited  $\text{H}^+$  conductance and/or uncoupling under physiological conditions, agonist-induced mitochondrial ATP production would be reduced. If, on the other hand, the physiological function of these UCPs is the result of mitochondrial  $\text{Ca}^{2+}$  uptake, overexpression of UCP2 and UCP3 should result in an enhanced mitochondrial ATP production on cell stimulation. Overexpression of either UCP2 or UCP3 elevated mitochondrial ATP synthesis on cell stimulation by  $70.9 \pm 11.5$  and  $111.9 \pm 31.7\%$ , respectively (see Supplementary Information,

Fig. S4c). These data further support the concept that UCP2 and UCP3 are essentially involved in mitochondrial  $\text{Ca}^{2+}$  sequestration on cytosolic  $\text{Ca}^{2+}$  elevation.

We have described a previously unknown physiological role for UCP2 and UCP3. For the first time, two proteins with known sequence are characterized as fundamental for mitochondrial  $\text{Ca}^{2+}$  uniport. Although, it remains unclear whether or not UCP2 and UCP3 represent the channel proteins responsible for mitochondrial  $\text{Ca}^{2+}$  sequestration, the characterization of these proteins as fundamental contributors to mitochondrial  $\text{Ca}^{2+}$  uniport provides unique possibilities for the elucidation of the mitochondrial  $\text{Ca}^{2+}$  uniport mechanisms, and to explore the physiological and pathological roles of this process.

## METHODS

### Animals

Mice breeding and experiments were performed according the standards established by the Austrian Federal Ministry of Education, Science and Culture, Division of Genetic Engineering and Animal Experiments (Vienna, Austria).

### Cell culture and transfection

The human umbilical vein endothelial cell line EA.hy926 (ref.16; passage 45–85), freshly isolated endothelial cells from the human umbilical vein (passage 2–4), CHO-K1 and HeLa cells were used in this study. Cells were isolated, cultured and transfected as previously described<sup>20</sup>.

### Plasmid construction for UCP overexpression

cDNAs encoding full-length human *UCP2* and *UCP3* were amplified by RT-PCR from total RNA from EA.hy926 cells<sup>16</sup>. The forward and reverse primers were: 5'-GGGGTACCGCAGGAAATCAGCATCATGG-3' and 5'-CCGCTCGAGTAGAGACAAAGCCAGAGGTG-3' for *UCP2* (positions 365 and 1353, respectively; GenBank accession no. NM\_003355); 5'-GGGGTACCGCAGAGCCTTCCAGGACTAT-3' and 5'-CCGCTCGAGTCTTGCTTGTTCAAAACGG-3' for *UCP3* (positions 186 and 1153, respectively; GenBank accession no. NM\_003356.2). Products were subcloned into the *KpnI*-*XhoI* sites of the EF-1 $\alpha$  multiple cloning site of the mammalian expression vector pBudCE4.1 (Invitrogen, Carlsbad, CA). For cytosolic free  $\text{Ca}^{2+}$  measurements, cells were transiently transfected with pBudCE4.1 containing either *UCP2* or *UCP3* cDNA in the EF-1 $\alpha$ -controlled multiple cloning site and mitochondria-targeted DsRed in the CMV-controlled multiple cloning site. For mitochondrial free  $\text{Ca}^{2+}$  measurements, mitochondria-targeted ratiometric pericam<sup>17</sup> was subcloned into the *HindIII*-*EcoRI* site of the CMV-MCS of UCP-containing vector. Targeting was analysed using UCP-sapphire fusion proteins in pBudCE4.1.

### Mutagenesis of UCPs

Amino acids 160–169 of human *UCP2* and amino acids 163–172 of human *UCP3* were replaced by glycines by PCR cloning. cDNAs of mutated *UCP* genes were cloned into the

pBudCE4.1. As for the wild-type UCPs, sapphire fusion proteins of all mutated UCPs were generated.

### Plasmid construction for UCP2 mRNA interference

pBU6 plasmid was constructed by replacing the CMV promoter of pBudCE4.1 by the U6 promoter of pSuppressor (Imgenex, Sorrento Valley, CA). To generate pBU6-UCP siRNA target sequence, oligonucleotides were designed that contained a unique 19-nucleotide double-stranded human *UCP* target sequence, present as an inverted repeat, separated by a loop of a 9-nucleotide spacer, and flanked by a 5-T RNA-polymerase III terminator sequence at the 3'-end. The matching strands were annealed to double-stranded DNA and inserted behind the U6 promoter of pBU6. The oligonucleotides against *UCP2* mRNA had the following sequence: 5'-

TCGAGGCCTGTATGATTCTGTCAAAGTTCTCTTGACAGAATCATAACAGGCCTTTT  
TC-3' and 5'-

CTAGGAAAAAGGCCTGTATGATTCTGTCAAGAGAACTTTGACAGAATCATAACAG  
GCC-3', respectively. The 19-nucleotide sequence corresponds to position 672–690 of *UCP2* (GenBank accession no. NM\_003355). Oligonucleotides that did not reduce the *UCP2* protein levels, and did not affect mitochondrial and/or cytosolic  $\text{Ca}^{2+}$  signalling in response to cell stimulation, were used as non-functional siRNA controls in all experiments in which siRNAs against either *UCP2* and/or *UCP3* were used. The sequences for these oligonucleotides were: 5'-

TCGAGTGCTGAGCTGGTGACCTAAAGTTCTCTTAGGTCACCAGCTCAGCACTTTT  
TC-3' and 5'-

CTAGGAAAAAGTGCTGAGCTGGTGACCTAAGAGAACTTTAGGTCACCAGCTCAG  
CAC-3', respectively. The 19-nucleotide sequence corresponds to position 952–970 of *UCP2* (GenBank acc. no. NM\_003355). Final plasmids containing the inserts were verified by restriction endonuclease digestion and automated fluorescent DNA sequencing. For silencing *UCP3* expression, double-stranded RNAs from Quiagen (Hilden, Germany) were used.

### Isolation of mitochondria from mouse liver and *Saccharomyces cerevisiae*

Mitochondria from liver of wild-type and *Ucp2*<sup>-/-</sup> mice, and yeast, were isolated according to Storrie and Madden<sup>21</sup> and Daum *et al.*<sup>22</sup>, respectively (see Supplementary Information, Methods).

### Ca<sup>2+</sup> measurements

Free cytosolic  $\text{Ca}^{2+}$  concentration was monitored ratiometrically as ratio signals at 340 nm and 380 nm excitation and 510 nm emission using fura-2 (ref. 23).

To monitor free mitochondrial  $\text{Ca}^{2+}$  concentration, cells were cotransfected with mitochondria-targeted ratiometric-pericam<sup>17</sup> and measured using a fluorescence microscope (Eclipse TE300, Nikon, Vienna, Austria) as previously described<sup>2,24</sup>. Due to the properties of the sensor, data presented are normalized to  $1-(F_{433}/F_0)$  and non-normalized values are shown in the Supplementary Information, Table S1.

Mitochondrial  $\text{Ca}^{2+}$  uptake from the medium was measured with Calcium Green-5N (0.1  $\mu\text{M}$ ; Molecular Probes Europe, Leiden, The Netherlands) according to previously described methods<sup>25</sup>. Isolated mitochondria (0.5 mg protein) were resuspended in 2 ml high KCl-buffer (110 mM KCl, 0.5 mM  $\text{KH}_2\text{PO}_4$ , 1 mM  $\text{MgCl}_2$ , 20 mM HEPES, 0.01 mM EGTA, 5 mM succinate, 0.004 mM rotenone at pH 7.2). Fluorescence was recorded at room temperature at 506 nm excitation and 532 nm emission (Hitachi F-4500; Inula, Vienna, Austria).  $F_{\text{min}}$  and  $F_{\text{max}}$  were established by addition of 1 mM EGTA and 10 mM  $\text{Ca}^{2+}$ . The  $K_D$  of Calcium Green-5N under the respective experimental conditions was 7.54 (6.62–8.59)  $\mu\text{M}$ .

Measurement of mitochondrial  $\text{Ca}^{2+}$  uptake in digitonin-permeabilized HeLa cells was performed in high KCl-buffer containing 1  $\mu\text{M}$  thapsigargin and  $2.5 \times 10^6$  cells per ml using Calcium Green-5N as described above. The plasma membranes were permeabilized by treatment with 3  $\mu\text{M}$  digitonin for 6 min.

$\text{Ca}^{2+}$  measurements in isolated single mitochondria were performed to previously described methods<sup>26</sup>. A 20  $\mu\text{l}$  drop of the suspension of fura-2-loaded mitochondria was placed on a coverslip and mounted onto the fluorescence microscope (Axiovert 200M; Zeiss, Vienna, Austria). After 8 min, attached mitochondria were perfused with assay buffer (20 mM HEPES, 130 mM KCl, 1 mM  $\text{MgCl}_2$ , 0.5 mM  $\text{KH}_2\text{PO}_4$ , 10 mM succinate, 2 mM malate, 0.5 mM EGTA, 0.6 mM ATP, 0.05 mM ADP at pH 7.2) at 2 ml per min.  $\text{Ca}^{2+}$  uptake into single mitochondria was monitored on changing the perfusion solution from  $\text{Ca}^{2+}$  free buffer to a buffer containing 10  $\mu\text{M}$  free  $\text{Ca}^{2+}$ .

Free  $\text{Ca}^{2+}$  concentration within the lumen of the endoplasmic reticulum  $\text{Ca}^{2+}$  was measured with D1 (ref. 27), as described previously<sup>28</sup>.

### **Confocal imaging, three-dimensional rendering and analysis of mitochondrial structural parameters**

For details of these experiments, please see Supplementary Information, Methods.

### **Immunoblotting analyses**

Western blot analysis was performed according to the methods described previously<sup>29</sup>.

### **ATP measurements**

Mitochondrial ATP synthesis was monitored in luciferase transfected cells. Further details are described in the Supplementary Information, Methods.

### **Supplementary Material**

Refer to Web version on PubMed Central for supplementary material.

### **Acknowledgments**

We thank: B. B. Lowell (Beth Israel Deaconess Medical Center and Harvard Medical School, Boston, MA) for providing the *Ucp2*<sup>-/-</sup> and *Ucp3*<sup>-/-</sup> mice; M. D. Brand (MRC Dunn Human Nutrition Unit, Cambridge, UK) for the yeast strains expressing UCP2 and UCP3; A. Miyawaki (Riken, Wako, Saitama, Japan) for mitochondria-



targeted ratiometric pericam; C. J. S. Edgell (University of North Carolina, Chapel Hill, NC) for the EA.hy926 cells; T. Pozzan (University Padova, Padova, Italy) for mitochondria-targeted DsRed; R. Tsien (University of California/San Diego, CA) for D1ER and YC4er; and R. Rizzuto (University Ferrara, Ferrara, Italy) for the luciferase construct. The excellent technical assistance of B. Petschar and A. Schreilechner, and the help of K. Osibow in designing cloning strategies are highly appreciated by the authors. We thank N. Demaurex and M. Frieden (University of Geneva, Geneva, Switzerland) for critical review of the manuscript. This work was supported by the Austrian Science Funds (P16860-B9; F3010-B05) and the Franz-Lanyar-Stiftung. The Institute of Molecular Biology and Biochemistry was supported by the infrastructure program of the Austrian ministry of education, science and culture.

## References

- Jouaville LS, Pinton P, Bastianutto C, Rutter GA, Rizzuto R. Regulation of mitochondrial ATP synthesis by calcium: evidence for a long-term metabolic priming. *Proc. Natl Acad. Sci. USA.* 1999; 96:13807–13812. [PubMed: 10570154]
- Malli R, Frieden M, Trenker M, Graier WF. The role of mitochondria for Ca<sup>2+</sup> refilling of the ER. *J. Biol. Chem.* 2005; 280:12114–12122. [PubMed: 15659398]
- Hoth M, Button DC, Lewis RS. Mitochondrial control of calcium-channel gating: a mechanism for sustained signaling and transcriptional activation in T lymphocytes. *Proc. Natl Acad. Sci. USA.* 2000; 97:10607–10612. [PubMed: 10973476]
- Parekh AB. Slow feedback inhibition of calcium release-activated calcium current by calcium entry. *J. Biol. Chem.* 1998; 273:14925–14932. [PubMed: 9614097]
- Gunter TE, Buntinas L, Sparagna G, Eliseev R, Gunter K. Mitochondrial calcium transport: mechanisms and functions. *Cell Calcium.* 2000; 28:285–296. [PubMed: 11115368]
- Duchen MR. Mitochondria and Ca<sup>2+</sup> in cell physiology and pathophysiology. *Cell Calcium.* 2000; 28:339–348. [PubMed: 11115373]
- Kirichok Y, Krapivinsky G, Clapham DE. The mitochondrial calcium uniporter is a highly selective ion channel. *Nature.* 2004; 427:360–364. [PubMed: 14737170]
- Brand MD, Esteves TC. Physiological functions of the mitochondrial uncoupling proteins UCP2 and UCP3. *Cell Metab.* 2005; 2:85–93. [PubMed: 16098826]
- Jezek P, Zackova M, Ruzicka M, Skobisova E, Jaburek M. Mitochondrial uncoupling proteins--facts and fantasies. *Physiol. Res.* 2004; 53:S199–S211. [PubMed: 15119950]
- Krauss S, Zhang CY, Lowell BB. The mitochondrial uncoupling-protein homologues. *Nat. Rev. Mol. Cell Biol.* 2005; 6:248–261. [PubMed: 15738989]
- Ricquier D, Bouillaud F. The uncoupling protein homologues: UCP1, UCP2, UCP3, StUCP and AtUCP. *Biochem. J.* 2000; 345:161–179. [PubMed: 10620491]
- Brand MD, et al. Mitochondrial superoxide: production, biological effects, and activation of uncoupling proteins. *Free Radic. Biol. Med.* 2004; 37:755–767. [PubMed: 15304252]
- Dejean L, Camara Y, Sibille B, Solanes G, Villarroya F. Uncoupling protein-3 sensitizes cells to mitochondrial-dependent stimulus of apoptosis. *J. Cell Physiol.* 2004; 201:294–304. [PubMed: 15334664]
- Krauss S, et al. Superoxide-mediated activation of uncoupling protein 2 causes pancreatic  $\beta$  cell dysfunction. *J. Clin. Invest.* 2003; 112:1831–1842. [PubMed: 14679178]
- Harper ME, et al. Decreased mitochondrial proton leak and reduced expression of uncoupling protein 3 in skeletal muscle of obese diet-resistant women. *Diabetes.* 2002; 51:2459–2466. [PubMed: 12145158]
- Edgell CJ, McDonald CC, Graham JB. Permanent cell line expressing human factor VIII-related antigen established by hybridization. *Proc. Natl Acad. Sci. USA.* 1983; 80:3734–3737. [PubMed: 6407019]
- Nagai T, Sawano A, Park ES, Miyawaki A. Circularly permuted green fluorescent proteins engineered to sense Ca<sup>2+</sup> Proc. Natl Acad. Sci. USA. 2001; 98:3197–3202. [PubMed: 11248055]
- Vidal-Puig AJ, et al. Energy metabolism in uncoupling protein 3 gene knockout mice. *J. Biol. Chem.* 2000; 275:16258–16266. [PubMed: 10748196]
- Yoshitomi H, Yamazaki K, Tanaka I. Cloning of mouse uncoupling protein 3 cDNA and 5'-flanking region, and its genetic map. *Gene.* 1998; 215:77–84. [PubMed: 9666083]

20. Malli R, et al. Sustained  $\text{Ca}^{2+}$  transfer across mitochondria is essential for mitochondrial  $\text{Ca}^{2+}$  buffering, store-operated  $\text{Ca}^{2+}$  entry, and  $\text{Ca}^{2+}$  store refilling. *J. Biol. Chem.* 2003; 278:44769–44779. [PubMed: 12941956]
21. Storrie B, Madden EA. Isolation of subcellular organelles. *Methods Enzymol.* 1990; 182:203–225. [PubMed: 2156127]
22. Daum G, Bohni PC, Schatz G. Import of proteins into mitochondria. Cytochrome b2 and cytochrome c peroxidase are located in the intermembrane space of yeast mitochondria. *J. Biol. Chem.* 1982; 257:13028–13033. [PubMed: 6290489]
23. Grynkiewicz G, Poenie M, Tsien RY. A new generation of  $\text{Ca}^{2+}$  indicators with greatly improved fluorescence properties. *J. Biol. Chem.* 1985; 260:3440–3450. [PubMed: 3838314]
24. Zoratti C, Kipmen-Korgun D, Osibow K, Malli R, Graier WF. Anandamide initiates  $\text{Ca}^{2+}$  signaling via CB2 receptor linked to phospholipase C in calf pulmonary endothelial cells. *Br. J. Pharmacol.* 2003; 140:1351–1362. [PubMed: 14645143]
25. Murphy AN, Bredesen DE, Cortopassi G, Wang E, Fiskum G. Bcl-2 potentiates the maximal calcium uptake capacity of neural cell mitochondria. *Proc. Natl Acad. Sci. USA.* 1996; 93:9893–9898. [PubMed: 8790427]
26. Vergun O, Reynolds IJ. Fluctuations in mitochondrial membrane potential in single isolated brain mitochondria: modulation by adenine nucleotides and  $\text{Ca}^{2+}$ . *Biophys. J.* 2004; 87:3585–3593. [PubMed: 15315954]
27. Palmer AE, Jin C, Reece JC, Tsien RY. Bcl-2-mediated alterations in endoplasmic reticulum  $\text{Ca}^{2+}$  analyzed with an improved genetically encoded fluorescent sensor. *Proc. Natl Acad. Sci. USA.* 2004; 101:17404–17409. [PubMed: 15585581]
28. Osibow K, Malli R, Kostner GM, Graier WF. A new type of non- $\text{Ca}^{2+}$ -buffering apo(a)-based fluorescent indicator for intraluminal  $\text{Ca}^{2+}$  in the endoplasmic reticulum. *J. Biol. Chem.* 2006; 281:5017–5025. [PubMed: 16368693]
29. Schaeffer G, et al. Intercellular signalling within vascular cells under high d-glucose involves free radical-triggered tyrosine kinase activation. *Diabetologia.* 2003; 46:773–783. [PubMed: 12811469]
30. Malli R, Frieden M, Osibow K, Graier WF. Mitochondria efficiently buffer sub-plasmalemmal  $\text{Ca}^{2+}$  elevation during agonist stimulation. *J. Biol. Chem.* 2003; 278:10807–10815. [PubMed: 12529366]

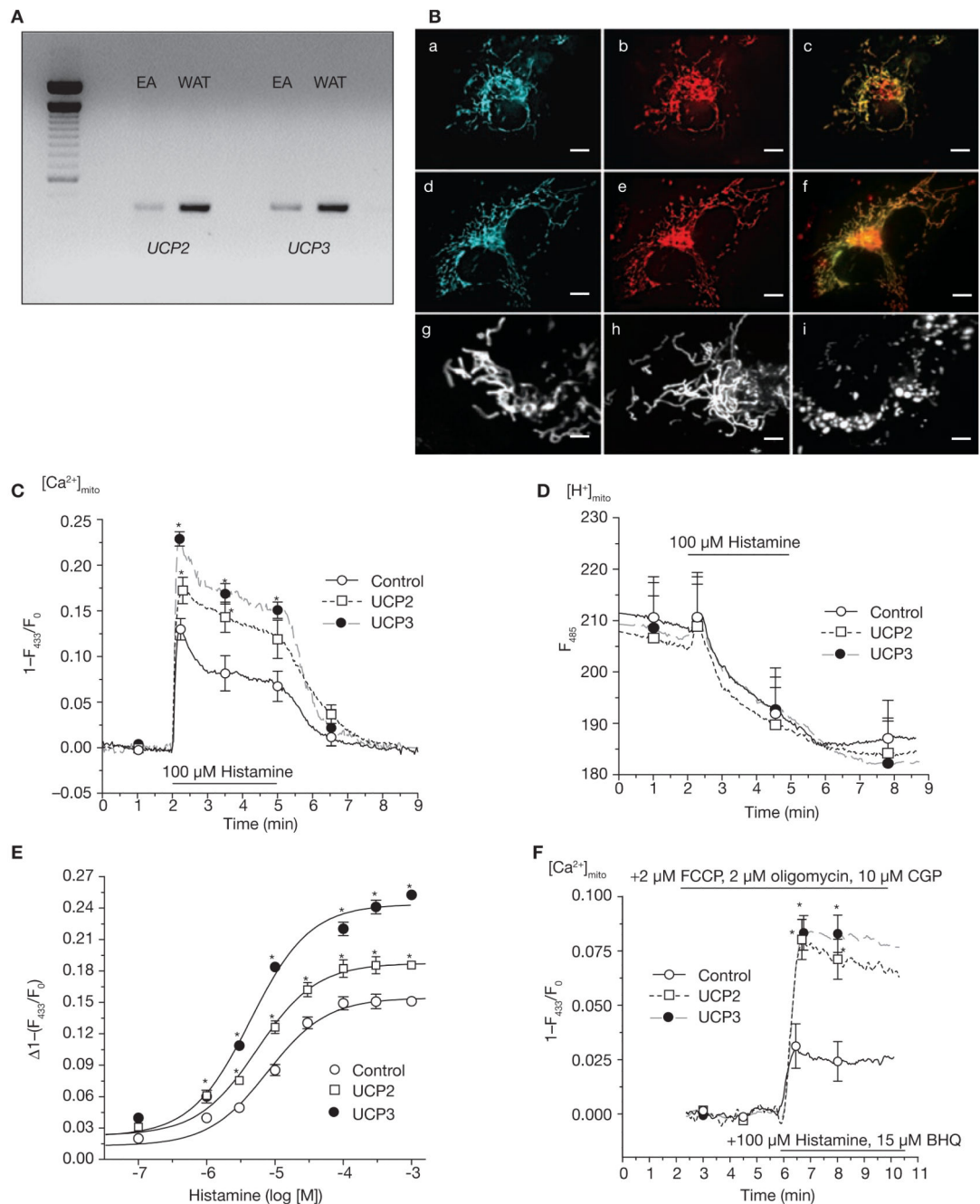


**Figure 1. Expression of UCP orthologues and functional tests on  $Ca^{2+}$  carrier function of UCP2 or UCP3 in human endothelial cells.**

(A) RT-PCR of *UCPs* in EA.hy926 (EA) cells and human white adipose tissue (WAT).

Methods and primer sequences are available shown in the Supplementary Information,

Methods. (B) Targeting of fusion proteins of UCP2 and UCP3; a and d show the localization

of the fusion constructs of UCP2 and UCP3; b and e the localization of mito-tracker orange;

and c and f the colocalization in the respective cell. Mitochondria structure was visualized in

endothelial cells transfected with mitochondria-targeted DsRed<sup>30</sup> (g) or DsRed and UCP2

alone (h). Further information is shown in the Supplementary Information, Fig. S1b. For

comparison with mitochondrial fragmentation, DsRed transfected cells were treated with 2  $\mu\text{M}$  FCCP for 5 min (i). The scale bars represent 10  $\mu\text{m}$  in a-f and 2  $\mu\text{m}$  in g-i. (C) UCP2 and UCP3 overexpression increased mitochondrial  $\text{Ca}^{2+}$  uptake. Mitochondrial  $\text{Ca}^{2+}$  elevation in response to 100  $\mu\text{M}$  histamine was measured with mitochondria-targeted ratiometric-pericam<sup>17</sup> in intact endothelial cells overexpressing the sensor, either alone (control;  $n = 32$ ) or together with UCP2 ( $n = 23$ ) or UCP3 ( $n = 18$ ). The asterisk indicates  $P < 0.05$  versus control. (D) UCP2 and UCP3 overexpression had no effect on histamine-induced changes in the mainly pH-sensitive wavelength of pericam ( $F_{485}$ ; data shown correspond to that shown in C). (E) UCP2 and UCP3 increased capacity, but not sensitivity, of mitochondrial  $\text{Ca}^{2+}$  uptake. Concentration response curves of histamine on mitochondrial  $\text{Ca}^{2+}$  elevation were obtained in single endothelial cells overexpressing mitochondria-targeted ratiometric pericam either alone (control,  $n = 6-12$ ) or together with UCP2 ( $n = 6-12$ ) or UCP3 ( $n = 6-12$ ). The asterisk indicates  $P < 0.05$  versus control. The respective data on cytosolic  $\text{Ca}^{2+}$  concentration are shown in the Supplementary Information, Fig. S1k. (F) UCP2 and UCP3 increased mitochondrial  $\text{Ca}^{2+}$  uptake independently of mitochondrial pH, mitochondrial  $\text{Na}^+-\text{Ca}^{2+}$  exchanger or mitochondrial membrane potential. In single endothelial cells overexpressing UCP2 ( $n = 11$ ) or UCP3 ( $n = 14$ ) mitochondria were depolarized by 2  $\mu\text{M}$  FCCP and 2  $\mu\text{M}$  oligomycin and the mitochondrial  $\text{Na}^+-\text{Ca}^{2+}$  exchanger was inhibited by CGP 37157, as described previously<sup>2</sup>. The asterisk indicates  $P < 0.05$  versus control ( $n = 14$ ). The error bars represent s.e.m.

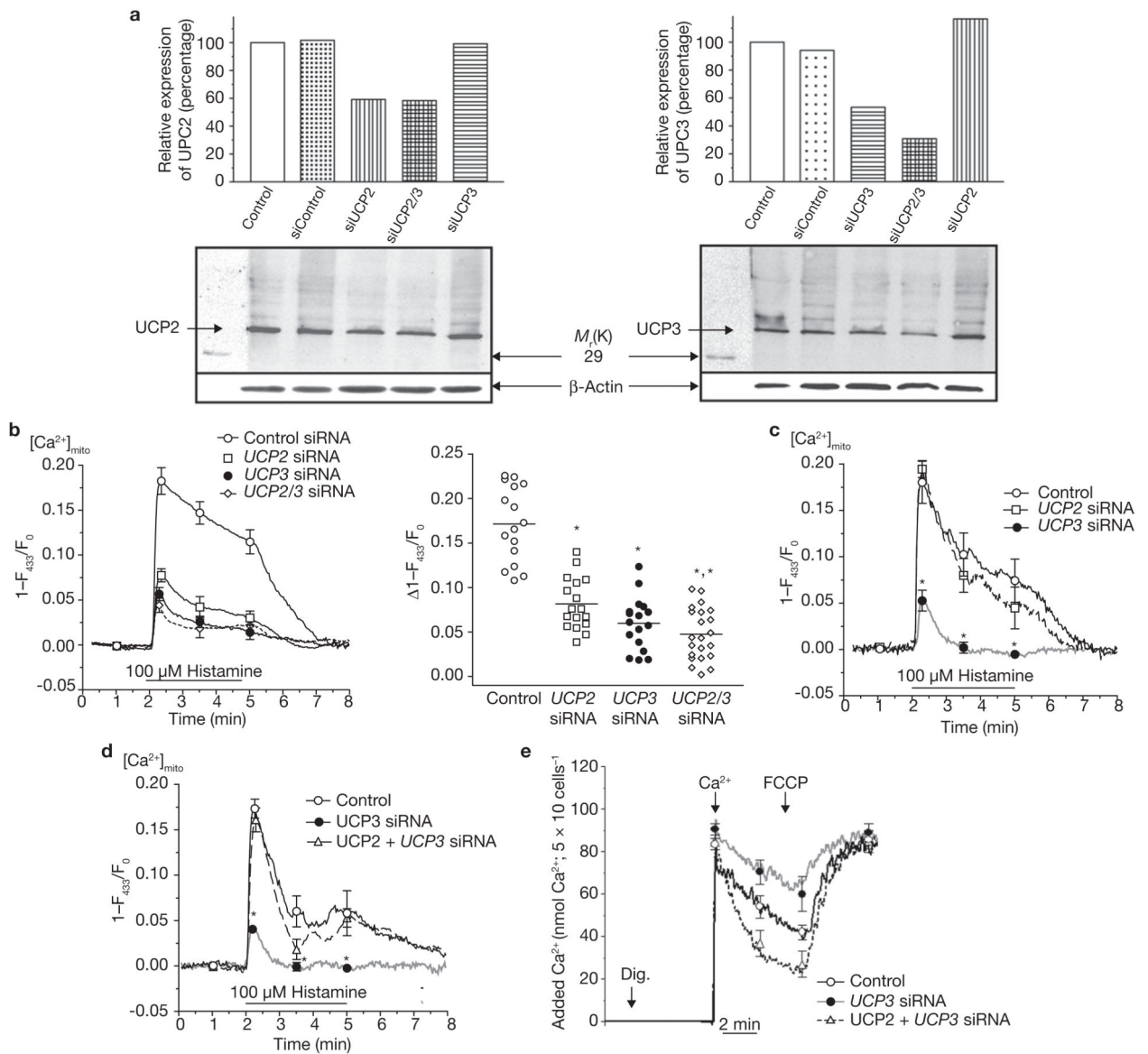


**Figure 2. UCP2 or UCP3 knockdown by siRNAs resulted in diminution and/or elimination of mitochondrial  $Ca^{2+}$  uptake.**

(a) siRNAs against *UCP2* or *UCP3* (see Supplementary Information, Fig. S2a) diminished expression of the respective protein, indicated by western blot analysis. The bars indicate the optical density of the respective band in lower panels, which are normalized according the corresponding  $\beta$ -actin band. Representative blots from three independent experiments are shown. (b) Silencing *UCP2* and/or *UCP3* expression attenuated and/or eliminated mitochondrial  $Ca^{2+}$  uptake. Mitochondrial  $Ca^{2+}$  sequestration in response to histamine was measured in single mitochondria-targeted ratiometric pericam-transfected endothelial cells that were cotransfected with control siRNA (see Supplementary Information, Methods), or with siRNAs against *UCP2* and/or *UCP3*. Average curves are shown on the left (control,  $n = 16$ ; *UCP2* siRNA,  $n = 17$ ; *UCP3* siRNA,  $n = 17$ ; and *UCP2/3* siRNA,  $n = 22$ ). The distribution of individual independent experiments is shown on the right. The bars indicate

the mean value. The single asterisk indicates  $P < 0.05$  versus control and the double asterisk indicates  $P < 0.05$  versus cells transfected with *UCP2* siRNA. The corresponding data on cytosolic free  $\text{Ca}^{2+}$  are provided in the Supplementary Information, Fig. S2b. **(c)** In single HeLa cells, which express *UCP3* but not *UCP2* (see Supplementary Information, Fig. S1a), only the *UCP3* siRNA ( $n = 14$ ) was suitable to prevent mitochondrial  $\text{Ca}^{2+}$  sequestration. The asterisk indicates  $P < 0.05$  versus control ( $n = 12$ ) and *UCP2* siRNA ( $n = 9$ ). **(d)** In single HeLa cells transfected with *UCP3* siRNA ( $n = 10$ ), overexpression of *UCP2* rescued mitochondrial  $\text{Ca}^{2+}$  uptake, as monitored with cotransfected mitochondria-targeted ratiometric-pericam. The asterisk indicates  $P < 0.05$  versus control ( $n = 11$ ) and *UCP2* + *UCP3* siRNA ( $n = 10$ ). **(e)** Overexpression of *UCP2* rescued mitochondrial  $\text{Ca}^{2+}$  uptake in suspended digitonin-permeabilized HeLa cells that were transfected with *UCP3* siRNA ( $n = 6$ ). Calcium Green-5N ( $0.1 \mu\text{M}$ ) was used to measure the reduction of extra-mitochondrial  $\text{Ca}^{2+}$  by mitochondria in digitonin-permeabilized and suspended HeLa cells, which were transiently transfected with either the vector alone (control), *UCP3* siRNA or *UCP2* + *UCP3* siRNA. As indicated (arrows),  $5 \mu\text{M}$  digitonin (Dig.),  $90 \text{ nmol}$   $\text{Ca}^{2+}$  and  $2 \mu\text{M}$  FCCP were added in the presence of  $1 \mu\text{M}$  thapsigargin. The asterisk indicates  $P < 0.05$  versus control ( $n = 6$ ) and *UCP2* + *UCP3* siRNA ( $n = 6$ ). The error bars represent s.e.m.

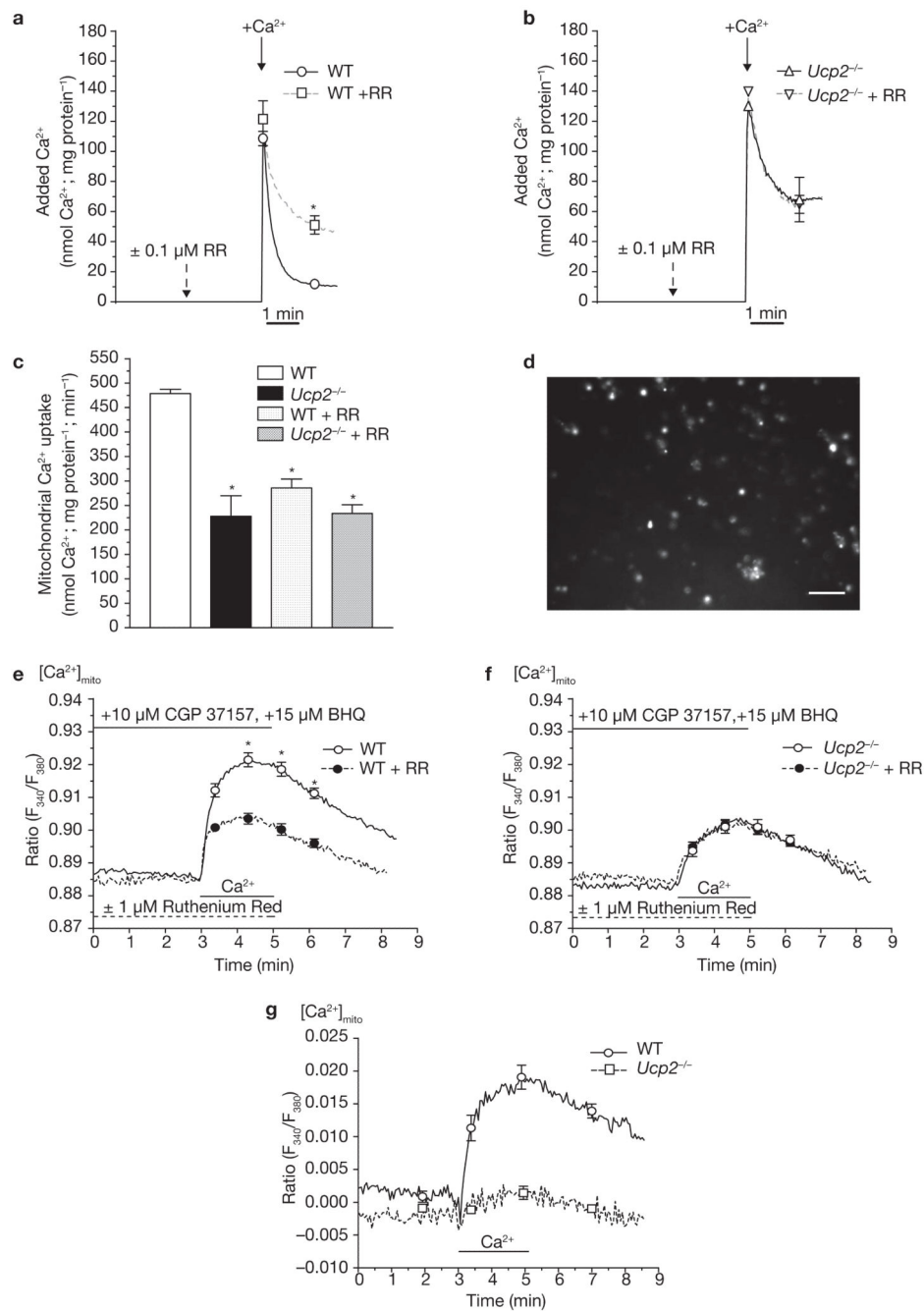


**Figure 3. In isolated liver mitochondria from  $Ucp2^{-/-}$  mice, no ruthenium red (RR)-sensitive  $\text{Ca}^{2+}$  uniporter exists.**

(a)  $\text{Ca}^{2+}$  uptake of suspended isolated liver mitochondria from wild-type (WT) animals was measured by monitoring the reduction of extra-mitochondrial  $\text{Ca}^{2+}$  on application of 140 nmol  $\text{Ca}^{2+}$  mg $^{-1}$  mitochondrial protein with Calcium Green-5N (0.1  $\mu\text{M}$ ). Experiments were performed in the absence ( $n = 7$ ) and presence (WT + RR,  $n = 4$ ; single asterisk indicates  $P < 0.05$  versus WT) of ruthenium red, an established inhibitor of mitochondrial  $\text{Ca}^{2+}$  uniporter (100 nM). (b) In suspended liver mitochondria isolated from  $Ucp2^{-/-}$  mice,  $\text{Ca}^{2+}$  uptake

(measured as described in **a**), was reduced ( $Ucp2^{-/-}$ ;  $n = 7$ ). The remaining  $Ca^{2+}$  uptake was insensitive to ruthenium red (100 nM;  $Ucp2^{-/-} + RR$ ;  $n = 4$ ). n.s. versus  $Ucp2^{-/-}$ . (**c**) Kinetics of mitochondrial  $Ca^{2+}$  uptake within 30 s after addition of  $Ca^{2+}$  calculated from the data presented in **a** and **b**. The asterisk indicates  $P < 0.05$  versus WT. (**d**) Fluorescence image of fura-2 loaded single mitochondria freshly isolated from mouse liver. The scale bar represents 10  $\mu m$ . (**e**) In isolated single liver mitochondria from wild-type animals, mitochondrial  $Ca^{2+}$  sequestration was measured in the absence (WT,  $n = 44$ ) and presence (WT + RR,  $n = 22$ ) of ruthenium red (1  $\mu M$ ) by mitochondrial fura-2. The asterisk indicates  $P < 0.05$  versus WT. (**f**)  $Ca^{2+}$  uptake in isolated single mitochondria from  $Ucp2^{-/-}$  mice measured by mitochondrial fura-2 was reduced ( $Ucp2^{-/-}$ ,  $n = 34$ ) compared with that obtained in the wild-type littermates. The remaining  $Ca^{2+}$  uptake into the liver mitochondria of  $Ucp2^{-/-}$  mice was not ruthenium red-sensitive ( $Ucp2^{-/-} + RR$ ,  $n = 21$ ). n.s. versus  $Ucp2^{-/-}$ . (**g**) Ruthenium red-sensitive mitochondrial  $Ca^{2+}$  uptake in single mitochondria freshly isolated from wild-type and  $Ucp2^{-/-}$  ( $Ucp2^{-/-}$ , asterisk indicates  $P < 0.05$  versus WT) mice calculated from data in **e** and **f**. The error bars represent s.e.m (**a–f**) or indicate 95% confidence intervals at the times shown (**g**).



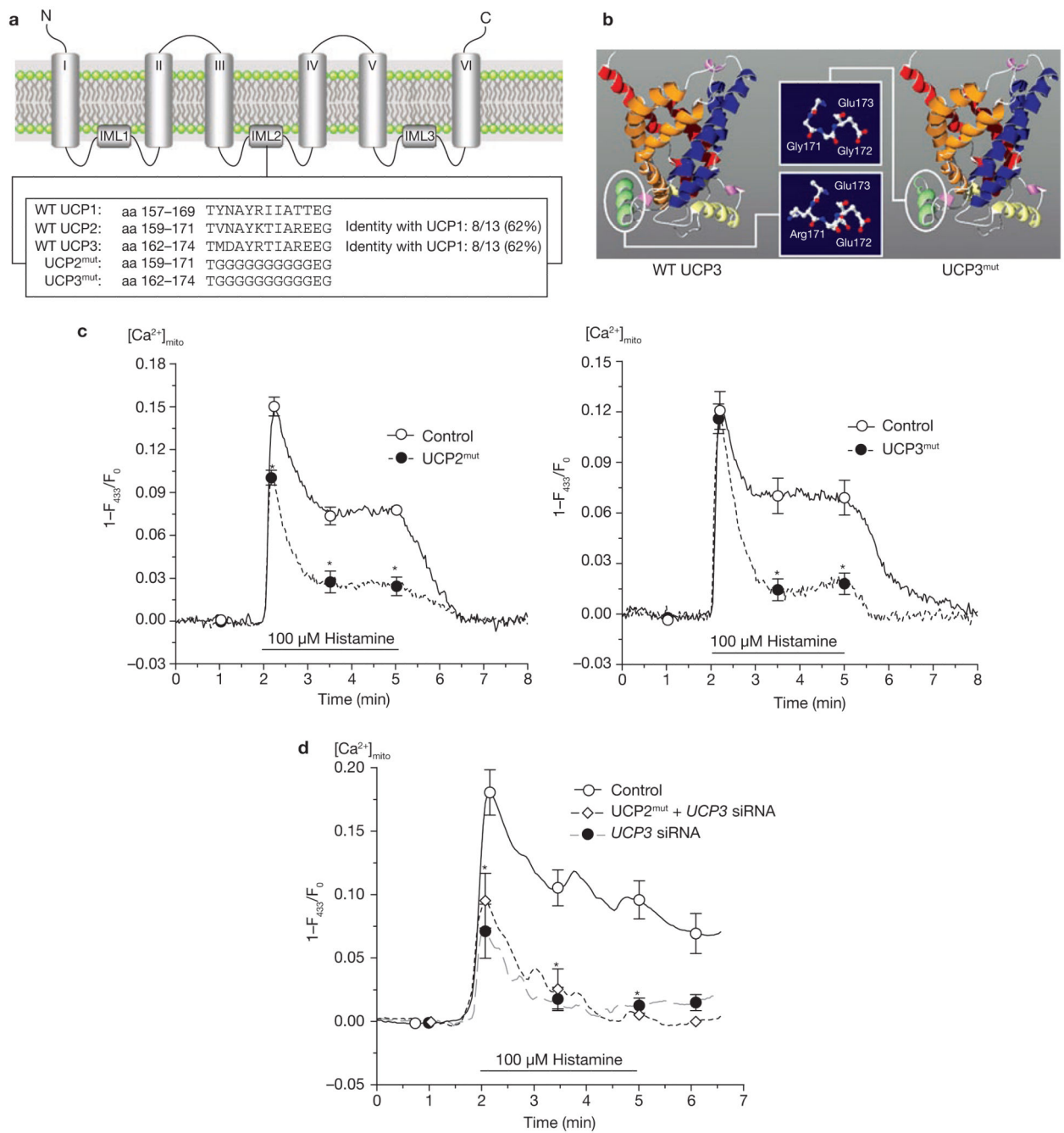


**Figure 4. Mutagenesis of UCP2 and UCP3 resulted in loss of  $\text{Ca}^{2+}$  function of the proteins and provided dominant-negative UCP homologues.**

(a) Sequence alignment and identification of specific domains common for UCP2 and UCP3, but not UCP1. Additional information is shown in the Supplementary Information.

(b) Using the ROBETTA full-chain protein structure prediction server (<http://robeta.bakerlab.org>), the protein structure of UCP2 and UCP3 was predicted to form a channel-like structure. As indicated, the mutation was introduced in a helix that is located on the matrix side of the inner mitochondrial membrane and results in shortening of the helix loop and loss of polarity. (c) Functional consequences on mitochondrial  $\text{Ca}^{2+}$  uptake in

single endothelial cells transiently expressing mitochondria-targeted ratiometric-pericam overexpressing mutated UCP2 ( $n = 25$ ) or mutated UCP3 ( $n = 15$ ). The asterisk indicates  $P < 0.05$  versus control ( $n = 17$ ). **(d)** Mutated UCP2 failed to rescue mitochondrial  $\text{Ca}^{2+}$  uptake in single HeLa cells transfected with *UCP3* siRNA. HeLa cells were transfected with either a non-functional control siRNA ( $n = 14$ ), *UCP3* siRNA ( $n = 9$ ) or *UCP3* siRNA together with mutated UCP2 ( $\text{UCP2}^{\text{mut}} + \text{UCP3}$  siRNA,  $n = 9$ ). Asterisk indicates  $P < 0.05$  versus control siRNA.